Journal of Alloys and Compounds 504 (2010) 186–191

Contents lists available at ScienceDirect

Journal of Alloys and Compounds

journal homepage: www.elsevier.com/locate/jallcom

Characterization of dislocation etch pits in HVPE-grown GaN using different wet chemical etching methods

Lei zhang, Yongliang Shao, Yongzhong Wu, Xiaopeng Hao*, Xiufang Chen, Shuang Qu, Xiangang Xu

State Key Lab of Crystal Materials, Shandong University, Jinan 250100, People's Republic of China

ARTICLE INFO

Article history:
Received 9 March 2010
Received in revised form 7 May 2010
Accepted 15 May 2010
Available online 27 May 2010

Keywords:
Dislocation
Etch pits
Hydride vapor phase epitaxy
GaN

ABSTRACT

The hydride vapor phase epitaxy (HVPE) grown GaN samples were etched by H_3PO_4, mixed solution of H_2SO_4 and H_3PO_4 (HH) and molten eutectic of KOH–NaOH (*E*), respectively. The etching characteristics and surface morphologies were studied by scanning electron microscopy (SEM) and atomic force microscopy (AFM). The density of etch pits obtained by *E* etching under optimum etching condition was around $3.0 \times 10^8\,cm^{-2}$, which was consistent with the results obtained by the cathodoluminescence (CL) investigation. Two types of etch pits with different sizes were all revealed on the GaN surface using different etching methods. The large etch pits were formed on screw or mixed dislocations, while small etch pits were formed on edge dislocations. The difference in the size of etch pits was interpreted by Cabrera's thermodynamic theory. Prolonging etching time, the morphology changes of etch pits were different by using H_3PO_4, HH and *E*. The etching rate by H_3PO_4 etching was the fastest and that by *E* etching was the slowest. According to these etching results, it could be concluded that *E* etching was a better method for evaluation of dislocations.

© 2010 Elsevier B.V. All rights reserved.

1. Introduction

In recent years, GaN have attracted a great interest due to their excellent properties for short wavelength optoelectronics and high-power high-frequency electronics [1–3]. However, GaN epitaxial layers have high dislocation densities ($10^8\,cm^{-2}$ to $10^{10}\,cm^{-2}$) due to the lattice mismatch and the difference in thermal expansion coefficient between GaN and the substrate [4]. The high dislocation density is harmful to the performance of optical and electrical devices. Homoepitaxy is the most effective method to reduce the dislocation density. However, due to the lack of native substrates, GaN has been mainly grown on foreign substrates [5,6]. To decrease the dislocation density of heteroepitaxial GaN, several techniques have been developed, such as epitaxial lateral overgrowth (ELOG) [7], overgrown on etch pits [8], fabrication of nanostructure on substrate [9]. The quality of GaN has been improved by using these methods, and correspondingly the dislocation density has been decreased. Therefore, it is necessary to study the dislocation of GaN epitaxial layers. Wet chemical etching method is commonly used for its merits of low cost, simple experimental procedure and no requirement of sample geometry [10]. Different etchants, such as phosphoric acid (H_3PO_4), mixed solution of H_2SO_4 and H_3PO_4 (HH), molten KOH and molten eutectic of KOH–NaOH (*E*), have been employed to study defects in GaN epitaxial layers [11–13]. However, few studies reported the differences of etching characteristics by using various wet chemical etching methods in detail.

In this paper, we investigated the differences in H_3PO_4, HH and *E* etching. The surface morphology of etched GaN epitaxial layers was observed by SEM and AFM. The etching parameters, morphology and mechanism of these systems were also investigated.

2. Experimental

GaN samples used for etching were grown by HVPE and they exhibited a Ga-polar surface. The thickness of GaN epitaxial layers was about 60 μm. The GaN samples were cut from the same wafer in order to ensure the comparability of the experiment results. To reveal the dislocation etch pits, the chemical etching was carried out by using H_3PO_4 (85%), HH (H_2SO_4:H_3PO_4 = 3:1) and *E* (NaOH:KOH = 51.5:48.5). In order to find optimal etching conditions of the GaN sample, we started at low temperature, and then gradually increased temperature or time of subsequent etching steps [13]. (1) H_3PO_4 etching: etching experiment in H_3PO_4 was performed from 210 °C to 250 °C. The glass container with H_3PO_4 solution was heated in a resistive heated oven. When the temperature of H_3PO_4 solution reached the specified value, GaN samples were immersed in the solution for 3–9 min, and then immediately taken out from the container and quenched in cool water to halt etching. (2) HH etching: the GaN samples were etched in HH for 3–12 min from 250 °C to 290 °C. The etching process was the same as H_3PO_4 etching. (3) *E* etching: a nickel crucible was used in the etching experiment. The molten KOH–NaOH liquid was heated to 370–470 °C for 3–10 min. Table 1 summarized the etching conditions and characteristics of HVPE-grown GaN using different wet chemical etching methods. AFM (Digital Instrument Dimension 3100) and SEM (Hitachi S-4800) were used to investigate the morphology of the as-grown and etched surface of GaN samples. CL investigations were performed using a Gatan MonoCL3 system attached to a Hitachi SU-70 SEM.

* Corresponding author. Tel.: +86 53188366218; fax: +86 53188364864.
E-mail address: xphao@sdu.edu.cn (X. Hao).

0925-8388/$ – see front matter © 2010 Elsevier B.V. All rights reserved.
doi:10.1016/j.jallcom.2010.05.085

Table 1
Etching conditions and characteristics of HVPE-grown GaN using wet chemical etching method.

Etchant	Etching temperature	Etching time	Etching characteristics	Figs.
H_3PO_4	210 °C	5 min	No change	–
	230 °C	3 min	Inverted hexagonal pyramid shape	Fig. 1(a)
		6 min	Hexagonal prism shape	Fig. 1(b)
		9 min	Huge etch pits	Fig. 1(c)
	250 °C	3 min	Huge etch pits	–
H_2SO_4:H_3PO_4 (3:1)	250 °C	5 min	No change	–
	270 °C	3 min	Large and small	Fig. 2(a)
		5 min	inverted hexagonal	Fig. 2(b)
		7.5 min	pyramid shape	–
		10 min		Fig. 2(c)
		12.5 min	Huge etch pits	–
	290 °C	3 min	Large inverted hexagonal pyramid shape	–
NaOH:KOH (51.5:48.5)	370 °C	6 min	A few etch pits	–
	420 °C	3 min	A few etch pits	Fig. 3(a)
		6 min	Large and small	Fig. 3(b)
		8 min	inverted hexagonal	Fig. 3(c)
		9.5 min	pyramid shape	Fig. 3(d)
	470 °C	3 min	Large hexagonal pyramid shape	–

3. Results and discussion

3.1. H_3PO_4 etching

When the GaN samples are etched by H_3PO_4 at 210 °C for 5 min, there is no change on their surfaces. Raising the etching temperature to 230 °C, etch pits with inverted hexagonal pyramid shape begin to emerge. Fig. 1(a–c) shows the surface morphology of etched GaN samples in H_3PO_4 at 230 °C for 3 min, 6 min and 9 min, respectively. After being etched for 3 min (Fig. 1(a)), two types of etch pits can be observed on the etched surface. One type is small dark dots less than 100 nm in diameter, and the other is large inverted hexagonal pyramid shape about 1 μm in diameter. The density of large etch pits is about 5.2×10^6 cm^{-2}. The shape of small dark dots is unclear and the density is about 1.1×10^8 cm^{-2}. The total density of the etch pits is 1.2×10^8 cm^{-2}. To verify the shape of small dark dots, AFM investigation was carried out. Fig. 2(a) illustrates the AFM image and section analysis of GaN etched at 230 °C for 3 min. It can be confirmed that the small dark dots in the SEM image of Fig. 1(a) are small etch pits with depth of about 5 nm. The shape of dark dots is also inverted hexagonal pyramid, which is the same as large etch pits. The depth of large etch pits is about 140 nm. Increasing the etching time, the small etching pits disappear, and the diameter of large etch pits increases from 1 μm (Fig. 1(a)) to 3–4 μm (Fig. 1(b)) and their shape changes from inverted hexagonal pyramid (Fig. 2(a)) to hexagonal prism structure (Fig. 2(b)). The morphology changes of etch pits indicate that overetching has occurred. The density of etch pits is 2.0×10^6 cm^{-2} in Fig. 1(b), which is two orders of magnitude less than that obtained in Fig. 1(a). When the etching time is increased to 9 min at 230 °C, some etch pits merges and forms huge etch pits with the diameter of 5–8 μm. Increasing the etching temperature to 250 °C, only huge etch pits are observed. So the optimum etching condition is 230 °C and 3 min.

3.2. HH etching

Etched by HH at 250 °C, the surface of the GaN sample remains unchanged. When the etching temperature reaches 270 °C, etch pits with inverted hexagonal pyramid shape are observed. The SEM

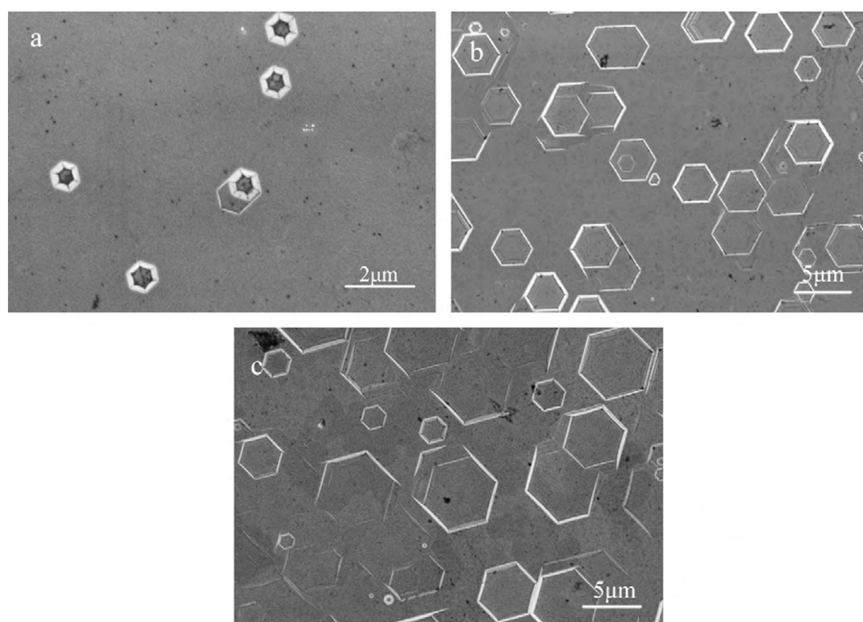

Fig. 1. SEM images of GaN samples etched in H_3PO_4 at 230 °C for 3 min (a), 6 min (b), 9 min (c).

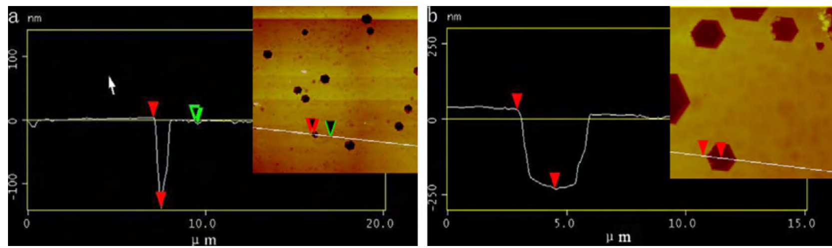

Fig. 2. AFM image and section analysis of etching pits formed in GaN sample after being etched in H_3PO_4 at 230 °C for 3 min (a) and 6 min (b).

images of the GaN sample etched by HH at 270 °C for 3–10 min are shown in Fig. 3. Two kinds of etch pits in different sizes are observed when the surface of GaN was etched with HH for 3 min (Fig. 3(a)). The densities of large etching pits and small ones are around 1.7×10^7 cm^{-2} and 1.8×10^8 cm^{-2}, respectively. The total density of the etch pits is 2.0×10^8 cm^{-2}. The AFM results (Fig. 3(d)) show the depths of the large and the small etch pits are about 120 nm and 7 nm, respectively. Further prolonging the etching time to 5 min, the diameter of large hexagonal etch pits increases from 800 nm to 1.5 μm, and that of small etch pits increases from 250 nm to 500 nm (Fig. 3(b)). The morphology of the two kinds of etch pits has no significant change except the increase in size. When the etching time prolongs to 10 min (Fig. 3(c)), the large and small etch pits begin to merge due to the increase in size. As a result, the estimated density of etch pits will decrease. When the etching is performed at 290 °C for 3 min, only large inverted hexagonal pyramid shape etch pits appear. The etching results show that the best etching parameters are 270 °C and 3 min because etch pits can be clearly identified and reliable dislocation density can be obtained under these conditions.

3.3. *E etching*

Etched by *E* at 370 °C for 6 min, only a few etch pits come out. After the etching temperature increased to 420 °C, a few etch pits are observed after 3 min (Fig. 4(a)), and the size of etch pits is very small and their shape cannot be identified. Six minutes later (Fig. 4(b)), two types of etch pits with different sizes appear. The average diameter of large etch pits is about 500 nm, while that of small etch pits is about 100 nm. The AFM results (Fig. 4(e)) show that the depths of the etch pits are about 120 nm and 30 nm, respectively. The hexagonal etch pits are well separated in space and can be clearly distinguished from their shape. The densities of the etching pits are around 4.2×10^7 cm^{-2} and 2.5×10^8 cm^{-2}, respectively. The total density of the etch pits is 3.0×10^8 cm^{-2}. After being etched for 8 min (Fig. 4(c)), the size of etch pits became twice as

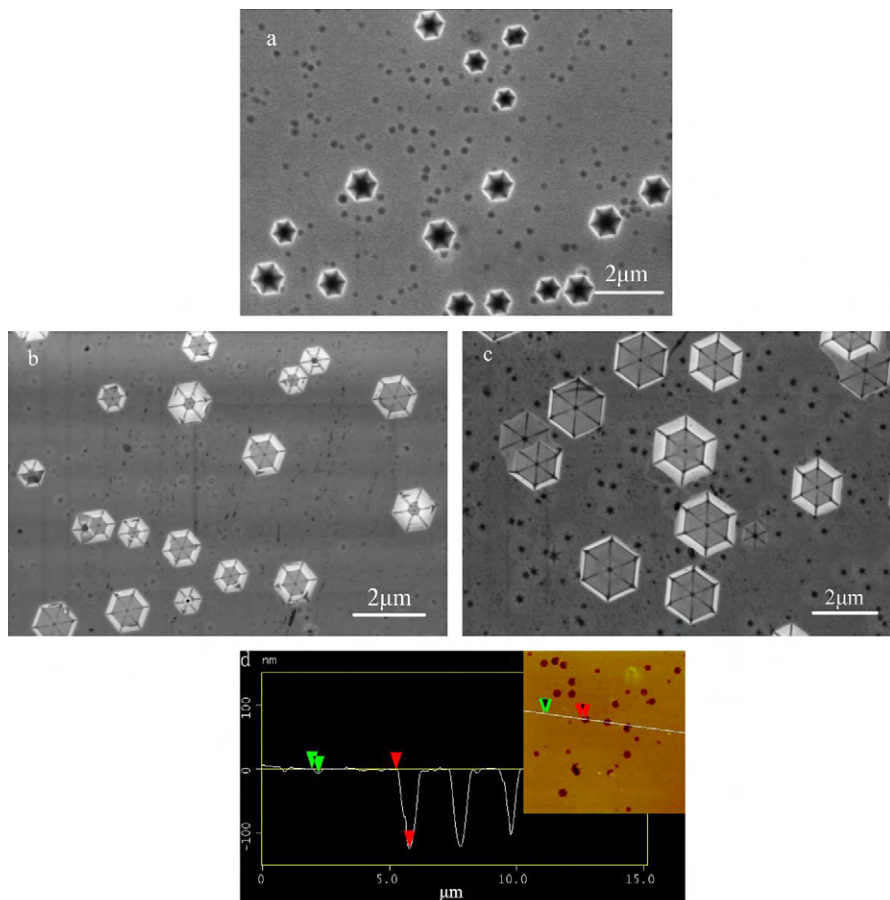

Fig. 3. SEM images of GaN samples etched in HH at 270 °C for 3 min (a), 5 min (b), 10 min (c). AFM image and section analysis of etching pits formed in GaN sample after being etched in HH at 270 °C for 3 min (d).

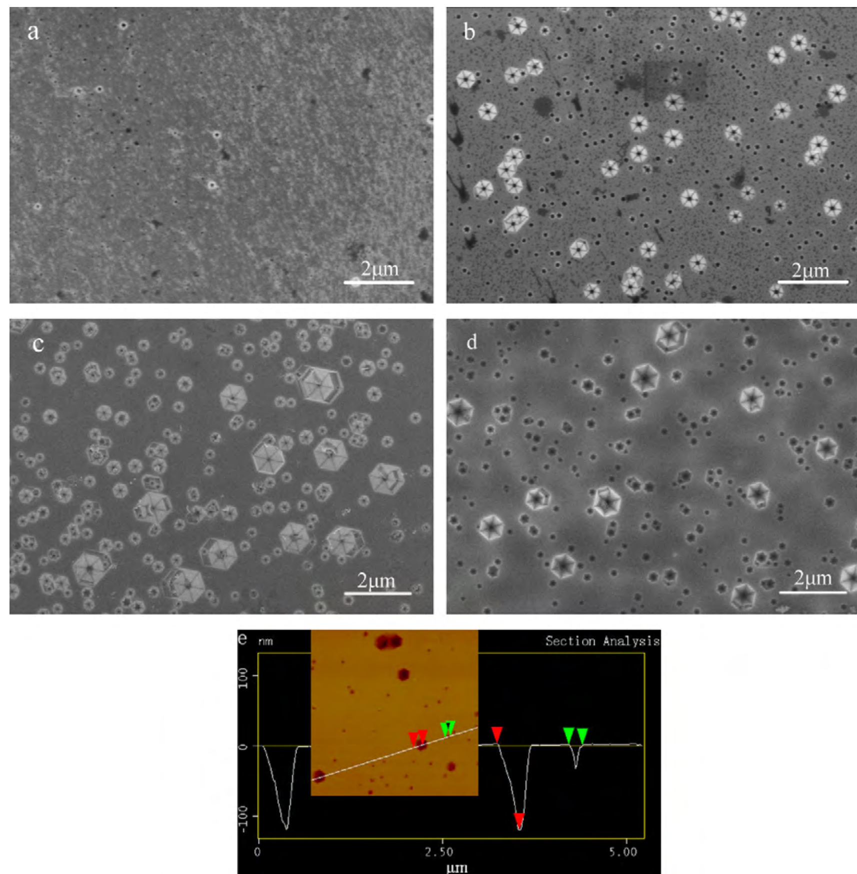

Fig. 4. SEM images of GaN samples etched in *E* at 420 °C for 3 min (a), 6 min (b), 8 min (c), 9.5 min (d); AFM image and section analysis of etching pits formed in GaN sample after being etched in *E* at 420 °C for 6 min (e).

big as that etched for 6 min (Fig. 4(b)). The size and shape of the etch pits do not change obviously when the etching time increased to 9.5 min (Fig. 4(d)). Further increasing the etching temperature to 470 °C, only large etch pits are observed. According to the etching results, it can be found that the optimum etching condition for revealing the defects for *E* is 420 °C and 6 min.

3.4. CL image

Fig. 5 shows a CL image for the as-grown HVPE GaN. The density of dark spots is about 3.0×10^8 cm^{-2}. The dark dots are corresponding to the non-radiative carrier recombination at dislocations, which is strongly localized due to the short-hole carrier diffusion length in GaN [14]. Therefore, the density of dark spot is close to the real density of dislocations. The density of etch pits obtained by *E* etching under the optimum etching conditions is around 3.0×10^8 cm^{-2}, which is consistent with the results obtained by the CL study. Therefore, it can be concluded that the density of dislocations obtained by *E* etching is reliable under the optimum etching conditions.

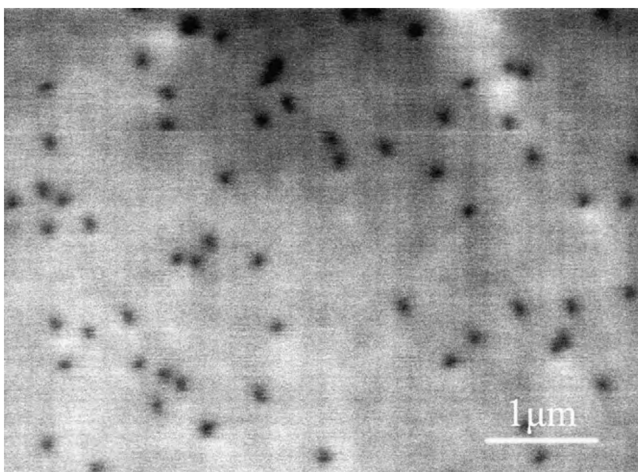

Fig. 5. CL image of the as-grown sample.

3.5. Discussion

In our investigation, two types of etch pits with different sizes are revealed on the GaN surface etched by different etchants. Visconti et al. obtained similar results using both molten KOH and H_3PO_4 etching on HVPE-grown GaN [15]. Chen et al. demonstrated that both large and small etch pits are formed by H_3PO_4 etching on MOCVD grown GaN, and the large etch pits are attributed to screw or mixed threading dislocations and the small ones to edge threading dislocations, according to their locations on the surface and Burgers vectors of threading dislocations [16]. Weyher et al. reported that three types of threading dislocations are revealed in molten *E* on HVPE-grown GaN by wet chemical etch, and the largest etch pits are formed on screw dislocations, intermediate size pits on mixed dislocations and the smallest ones on edge dislocations [13]. However, it is difficult to distinguish the largest etch pits and intermediate ones on the basis of our etching results. Therefore, by comparing the size and shape of etch pits, it can be concluded that the large etch pits are formed on screw or mixed dislocations, while small etch pits are formed on edge dislocations. Different sizes of etch pits could be interpreted in terms of Cabrera's thermodynamic

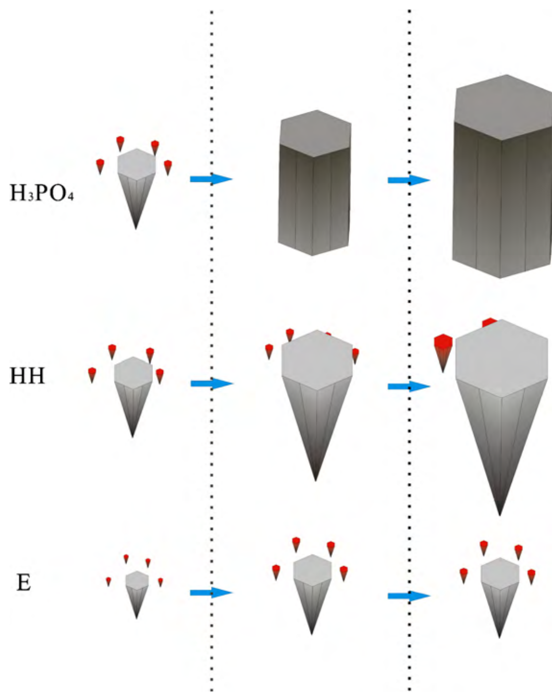

Fig. 6. Schematic diagram of the morphology change of etch pits using H_3PO_4, HH and *E*.

theory [17,18]. According to this theory, the energy localized in the vicinity of a dislocation lowers the free energy required for the nucleation of a cavity of unit depth in the surface at the site of the dislocation. This decrease in the free energy is the cause of preferred dissolution of the surface at the emergence points of dislocations. The free energy change associated with the formation of an etch pit at the dislocation site, ΔE, is given by:

$$\Delta E = 2\pi h r \gamma - \frac{\pi h r^2 \Delta\mu}{\Omega} - h\frac{Gb^2}{4\pi}\alpha \ln\left(\frac{r}{r_0}\right), \qquad (1)$$

where r is the radius of etch pit, h is the height of etch pit, r_0 is the radius of the dislocation core, $\Delta\mu$ is the change in free energy during dissolution (chemical potential), Ω is the molecular volume, γ is the specific surface free energy of an atom or molecule going from the solid surface into the solution, G is the shear modulus of the crystal, b is the Burgers vector of dislocation and α is the surface entropy factor. The sequence of Burgers vector of screw dislocation, edge dislocation and mixed dislocation in GaN epitaxial layers with wurtzite lattice is as follows: mixed dislocation > screw dislocation > edge dislocation. From Eq. (1) it can be concluded that the higher is the Burgers vector of dislocation, the lower is the value of ΔE. Consequently, dislocation etch pits are formed more easily on screw or mixed dislocation. The edge dislocations are more resistant to chemical etching due to the higher ΔE. Therefore, the size of screw or mixed dislocation etch pits is larger than that of edge dislocations.

Prolonging etching time, the morphology changes of etch pits are different by using H_3PO_4, HH and *E* etching at their respective optimum etching temperatures. The schematic diagram of the morphology change of the etch pits using H_3PO_4, HH and *E* is shown in Fig. 6. For H_3PO_4 etching, the shape of the etch pits change from the inverted hexagonal pyramid to hexagonal prism structure. Both diameter and depth of etch pits increase. For HH etching, some neighboring defects merge and form larger pits because of the size of the etch pits increased. For *E* etching, the size of etch pits increases at first, then did not change continuously. The size of etch pits etched by H_3PO_4 is the largest, while that etched by *E* is the smallest. This phenomenon indicates that the etch rate in GaN epilayer are different by using different etchants. Within the same etching time, the etching rate of H_3PO_4 is the fastest, while *E* is the slowest. It has been reported that the reactions using H_3PO_4 and *E* etchants during etching are as follows:

In H_3PO_4 [19]:

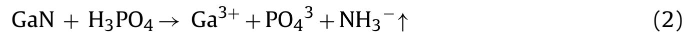

$$GaN + H_3PO_4 \rightarrow Ga^{3+} + PO_4{}^{3} + NH_3{}^{-}\uparrow \qquad (2)$$

In *E* [20]:

$$GaN + 3H_2O \xrightarrow{KOH,NaOH} Ga(OH)_3 + NH_3\uparrow \qquad (3)$$

According to the reaction (2), we tentatively assume the reaction using HH etchant is as follows:

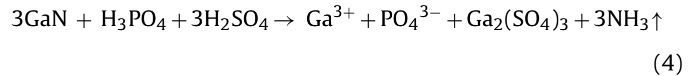

$$3GaN + H_3PO_4 + 3H_2SO_4 \rightarrow Ga^{3+} + PO_4{}^{3-} + Ga_2(SO_4)_3 + 3NH_3\uparrow \qquad (4)$$

From reaction (3), it can be found that $Ga(OH)_3$ are produced in the *E* etching. Some early reports showed that GaN could be etched in an sodium hydroxide (NaOH) aqueous solution, however, etching ceased upon the formation of an insoluble coating of presumably gallium hydroxide ($Ga(OH)_3$) [21,22]. Therefore, it can be considered that the morphology change of etch pit by *E* is related to $Ga(OH)_3$. At first, the amount of $Ga(OH)_3$ is limited and the etching is continuing, and the size of large and small etch pits increase. With increasing the etching time, when the amount of $Ga(OH)_3$ on the etched surface of GaN become more and more, the etching will cease. Oshima and Dwikusuma [23,24] reported H_2SO_4 etching of β-Ga_2O_3 crystal and sapphire, which was disturbed by the formation of insoluble sulfates ($Ga_2(SO4)_3$, $Al_2(SO_4)_3$). The etch rate of H_2SO_4 (<0.001 μm/min) is lower than that of H_3PO_4 (0.013–3.2 μm/min) [25], which may be due to the formation of insoluble $Ga_2(SO_4)_3$. From reaction (4), it can be seen that $Ga_2(SO_4)_3$ are formed in the HH etching. Therefore, the etch rate of the mixture of H_3PO_4 and H_2SO_4 is lower than H_3PO_4. As a result, *E* etching is prone to avoid merging of etch pits and well defined etch pits can be obtained within the same etching time. The overetching is more liable to occur with H_3PO_4 and HH etching. Correspondingly, the density of dislocation will be underestimated. From the above analysis, it can be seen that *E* etching is easier to control and can objectively reflect the density of dislocation. Therefore, it can be concluded that *E* etching is a better method for the evaluation of dislocations.

According to our etching results, the dislocation density of GaN grown on sapphire is very high (3.0×10^8 cm^{-2}). To decrease the dislocation density, we are trying to use pattern substrate and SiC substrate which could reduce the residual stress and lattice mismatch, and some good results are achieved. The efforts on decrease dislocation density are being carried out.

4. Conclusions

In summary, the etching characteristics of GaN surface by using H_3PO_4, HH and *E* were investigated. The density of dislocations obtained by *E* etching was reliable under the optimum etching conditions by the CL study. Two kinds of distinctive etch pits were revealed by these etchants, and the large etch pits were formed on screw or mixed dislocations, while small etch pits were formed on edge dislocations. Difference in the size of the etch pits was interpreted by Cabrera's thermodynamic theory. In addition, the change of the surface morphology along with time was also investigated. These changes were attributed to the difference of etching rate. The etching results indicated that the *E* etching was a better method for the evaluation of dislocations.

Acknowledgements

This work was supported by NCET, NSFC (contract no. 50823009, 50721002, 50801042), National “863” High Technology Plan (grant no. 2007AA03Z405). National Basic Research Program of China (973 Program) (2009CB930503), the Key Project of Chinese Ministry of Education (no. 109096).

References

[1] D. Ehrentraut, Z. Sitar, MRS Bull. 34 (2009) 259–265.
[2] H.Q. Jia, L.W. Guo, W.X. Wang, H. Chen, Adv. Mater. 21 (2009) 1–6.
[3] D.G. Zhao, D.S. Jiang, J.J. Zhu, H. Wang, Z.S. Liu, S.M. Zhang, Y.T. Wang, Q.J. Jia, H. Yang, J. Alloys Compd. 489 (2010) 461–464.
[4] J.L. Weyher, H. Ashraf, P.R. Hageman, Appl. Phys. Lett. 95 (2009) 031913.
[5] S. Qu, S. Li, Y. Peng, X. Zhu, X. Hu, C. Wang, X. Chen, Y. Gao, X. Xu, J. Alloys Compd. (2008), doi:10.1016/j.jallcom.2010.04.185.
[6] J Zou, W.D. Xiang, J. Alloys Compd. 484 (2009) 622–625.
[7] H.H. Huang, C.L. Chao, T.W. Chi, Y.L. Chang, P.C. Liu, L.W. Tu, J.D. Tsay, H.C. Kuo, S.J. Cheng, W.I. Lee, J. Cryst. Growth 311 (2009) 3029–3032.
[8] W. Zhang, Q.Y. Hao, C.C. Liu, Y.C. Feng, J. Alloys Compd. 456 (2008) 368–371.
[9] C.L. Chao, C.H. Chiu, Y.J. Lee, H.C. Kuo, P.C. Liu, J.D. Tsay, S.J. Cheng, Appl. Phys. Lett. 95 (2009) 051905.
[10] D. Zhuang, J.H. Edgar, Mater. Sci. Eng. R 48 (2005) 1–46.
[11] D.S. Peng, Y.C. Feng, H.B. Niu, J. Alloys Compd. 476 (2009) 629–634.
[12] J.Q. Liu, J.F. Wang, Y.F. Liu, K. Huang, X.J. Hu, Y.M. Zhang, Y. Xu, K. Xu, H. Yang, J. Cryst. Growth 311 (2009) 3080–3084.
[13] J.L. Weyher, S. Lazar, L. Macht, Z. Liliental-Weber, R.J. Molnar, J. Cryst. Growth 305 (2007) 384–392.
[14] S.J. Rosner, G. Girolami, Appl. Phys. Lett. 74 (1999) 2035–2037.
[15] P. Visconti, K.M. Jones, M.A. Reshchikov, R. Cingolani, H. Morkoc, Appl. Phys. Lett. 77 (2000) 3532–3534.
[16] J. Chen, J.F. Wang, H. Wang, J.J. Zhu, S.M. Zhang, D.G. Zhao, D.S. Jiang, H. Yang, U. Jahn, K.H. Ploog, Semicond. Sci. Technol. 21 (2006) 1229–1235.
[17] K. Samgwal, J. Mater. Sci. 17 (1982) 2227–2238.
[18] S. Mukerji, T. Kar, Jpn. J. Appl. Phys. 38 (1999) 832–837.
[19] M.G. Mynbaeva, Yu.V. Melnik, A.K. Kryganovskii, K.D. Mynbaevm, Electrochem. Solid State Lett. 2 (1999) 404–406.
[20] J.L. Weyher, L. Macht, Eur. Phys. J. Appl. Phys. 27 (2004) 37–41.
[21] T.L. Chu, J. Electrochem. Soc. 118 (1971) 1200.
[22] J.I. Pankove, J. Electrochem. Soc. 119 (1972) 1118.
[23] T. Oshima, T. Okuno, N. Arai, Y. Kobayashi, S. Fujita, Jpn. J. Appl. Phys. 48 (2009) 040208.
[24] F. Dwikusuma, D. Saulys, T.F. Kuech, J. Electrochem. Soc. 149 (2002) G603.
[25] D.A. Stocker, E.F. Schubert, Appl. Phys. Lett. 73 (1998) 2654–2656.